

# Energy performance prediction of thermoelectric ceiling radiant panels with a dedicated outdoor air system

Hansol Lim<sup>1</sup>, Janghoon Shin<sup>1</sup>, Shiyong Li<sup>1</sup>, Hye-Jin Cho<sup>1</sup> and Jae-Weon Jeong<sup>\*,1</sup>

*1 Department of Architecture Engineering, College of Engineering, Hanyang University,  
222 Wangsimni-Ro, Seungdong-Gu, Seoul, 04763, Republic of Korea*

*\*Corresponding author: [jjwarc@hanyang.ac.kr](mailto:jjwarc@hanyang.ac.kr)*

## ABSTRACT

This paper proposes a dedicated outdoor air system (DOAS) with thermoelectric module radiant cooling panels (TEM-RCP). The DOAS involves the concept of a decoupled system with a parallel sensible cooling unit. This concept implies decoupling of ventilation and air-conditioning functions. The DOAS treats latent loads from outside air intake as a 100 % OA ventilation system. Additionally, a parallel sensible cooling unit, such as ceiling radiant cooling panel (CRCP), generally removes sensible loads. In the study, the variable air volume system and DOAS CRCP using chilled water were also considered as a conventional HVAC system and traditional parallel cooling unit of DOAS, respectively. The two cases were compared to investigate the possibility of applying TEM-RCP on DOAS. Mathematical simulation models were developed, and the operating and annual energy consumptions for all three cases were estimated. The results indicated that the thermal performance was satisfied in all cases including the proposed systems. The proposed system resulted in annual energy consumption savings of 44.5 % when compared with the variable air volume system. On the other hands, the energy consumption of TEM-RCP exceeded that of the CRCP by 33 % due to its low coefficient of performance (COP) and additional energy from heat rejection. The proposed system did not exhibit benefits in terms of energy consumption when compared with that of the DOAS CRCP. However, it could be easily controlled by using input current without refrigerants and still continue to display energy saving potential when compared with the VAV system.

## KEYWORDS

Dedicated outdoor air system; radiant cooling; cooled ceiling; thermoelectric modules

## 1 INTRODUCTION

A decoupled system concept of a dedicated outdoor air system (DOAS) with parallel sensible cooling is used due to benefits including energy conservation and indoor air quality. The DOAS effectively accommodates latent loads and part of sensible loads. The system uses 100 % outside air with a minimum air flow rate for ventilation integrated with a parallel cooling unit, such as ceiling radiant cooling panel (CRCP), to remove sensible loads. A CRCP is an efficient way to achieve occupant thermal comfort and is generally used with metallic ceiling water panels. The coolant of this system involves water chilled by a vapor compression system that uses refrigerants. This system exhibits good efficiency. However, a concern involving the depletion of the ozone layer by refrigerants such as CFCs persists (Kim et al., 2016).

Hence, a thermoelectric module (TEM) is studied as a non-vapor compression technique without a refrigerant. Previous studies developed an air-cooled type TEM radiant cooling panel (TEM-RCP) and investigated its performance (Tan and Zhao, 2015). Nevertheless, there is a paucity of investigations examining the use of a TEM-RCP combined with a HVAC system. Additionally, previous studies did not focus on the use of a water-cooled type TEM-RCP given considerations to reduce system size. However, a water-cooled type exhibits better efficiency when compared to an air-cooled type with respect to aspects involving heat rejection (Lee, 2017). Therefore, the present study proposed a water-cooled type TEM-RCP

for parallel sensible cooling in DOAS. The study developed mathematical simulation models for DOAS TEM-RCP and CRCP systems. Furthermore, a variable air volume (VAV) system was simulated as a case for conventional HVAC system for comparison purposes. Finally, annual energy consumptions of both systems were compared to evaluate the possibility of applying TEM-RCP on a DOAS system.

## 2 SYSTEM DESCRIPTION

### 2.1 Variable air volume system

As shown in figure 1, a conventional VAV system was selected to compare operating energy consumption in a cooling season with a decoupled system involving a DOAS with a parallel cooling unit. In the VAV, the air flow rate is determined based on a sensible and latent load. Therefore, fan energy also varies with loads. In a cooling season, a dehumidification process occurs at the cooling coil and reheats air by using a heating coil to satisfy supply air temperature. Additionally, an enthalpy based economizer is used in the intermediate season.

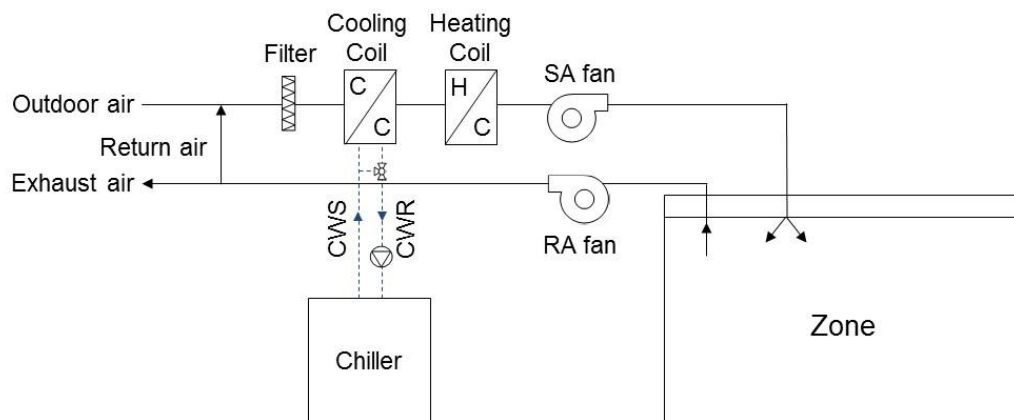


Figure 1: Schematic of a conventional VAV system

### 2.2 Dedicated outdoor air system with a chilled water ceiling radiant panel

The conventional DOAS considered in this study is shown in Figures 2 and 3. The DOAS consists of an enthalpy wheel, a sensible wheel, and a cooling coil. In the DOAS, a minimum ventilation air flow rate is supplied irrespective of the load. The enthalpy wheel reduces the work of the cooling coil by exchanging water and heat with exhaust air without mixing. The remaining latent load is removed at the cooling coil, and the sensible wheel reheats the supply air. Additionally, the CRCP that uses chilled water is used to accommodate the sensible load that remains after the DOAS satisfies the whole latent load and a part of the sensible load as shown in Figure 2. In this study, a single electric chiller was simulated to supply chilled water for the cooling coil and CRCP. A detailed operation mode of the DOAS is described in a previous study (Kim et al., 2016).

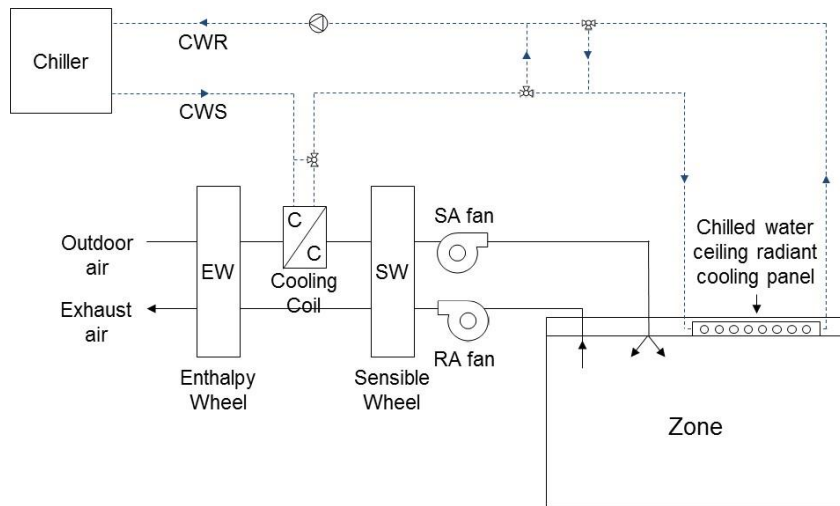


Figure 2: Schematic of DOAS with a chilled water ceiling radiant cooling panel

### 2.3 Dedicated outdoor air system with a thermoelectric module ceiling radiant panel

The configuration of the third case was similar to that of case in chapter 2.2 with the exception of the parallel cooling unit. The TEM RCP was used to investigate the energy potential of the TEM as a parallel cooling unit. The water-cooled type was selected to cool the hot side of TEM, and chilled water was supplied by using a cooling tower. Therefore, this system includes a chiller and cooling tower (Figure 3). A detailed configuration of the water-cooled TEM RCP is shown in figure 4. The cold side of TEMs was bonded to a thin aluminum panel with insulation to prevent heat conduction from the hot side to the cold side of the TEMs. The hollow metallic blocks were termed as water blocks, and they possess fins inside with high thermal conductivity that were bonded for heat removal on the hot side of the TEMs.

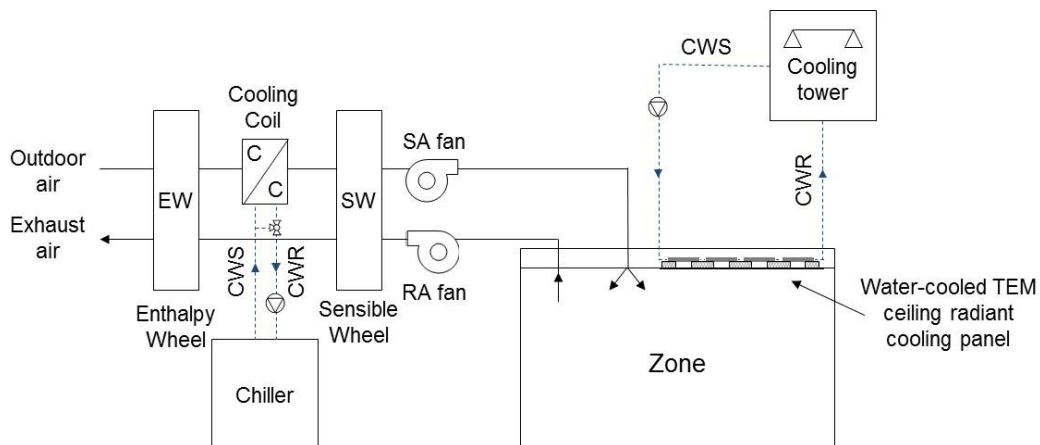


Figure 3: Schematic of DOAS with a water-cooled TEM radiant cooling panel

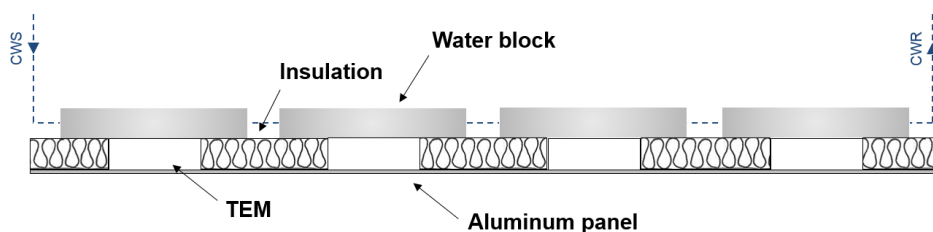


Figure 4: The configuration of the water-cooled TEM radiant cooling panel

### 3 SIMULATION OVERVIEW

#### 3.1 Model space

The sensible and latent loads of the design space were derived by using TRNSYS 17. The design space involved a floor area of 100 m<sup>2</sup> with a height of 3 m. Two windows with an area corresponding to 10 m<sup>2</sup> were located on the south and west exterior walls. The selected window-to-wall ratio corresponded to 0.17. The sensible and latent heat generation rates of an occupant were set as 75 W and 45 W, respectively, based on ASHRAE Standard 90.1. Typical occupancy and system schedules for an office building were applied to derive the typical loads for the model space. The set points of indoor temperature and relative humidity corresponded to 25 °C and 50 %, respectively for the cooling mode and 20 °C for heating mode, respectively. All U-values for the roof, ceiling, wall, and windows were selected based on local criteria.

#### 3.2 DOAS components

In the DOAS simulation, a polynomial empirical model for an enthalpy wheel was used to predict the efficiency of wheel as shown in Eq. (1) and (2) based on previous studies (Jeong et al., 2003; Jeong and Mumma, 2005). The temperature ( $T_{SA,in}$ ) and relative humidity ( $RH_{SA,in}$ ) of supply air, the face velocity of incoming supply air ( $V_{SA,in}$ ), and the ratio of exhaust air to outdoor air flow rate ( $Q_R$ ) were used to predict sensible effectiveness. Additionally, two factors, namely temperature ( $T_{EA,in}$ ) and relative humidity ( $RH_{EA,in}$ ) of exhaust air, were added to estimate the latent effectiveness as follows:

$$\varepsilon_{sen,max} = f(V_{SA,in}, T_{SA,in}, RH_{SA,in}, Q_R) \quad (1)$$

$$\varepsilon_{lat,max} = f(T_{SA,in}, T_{EA,in}, RH_{SA,in}, RH_{EA,in}, Q_R, V_{SA,in}) \quad (2)$$

The maximum values of sensible and latent effectiveness were assumed as 80 % to prevent the occurrence of impractical results. A speed control was necessary to adjust the humidity ratio of supply air ( $W_{SA,set}$ ) when the humidity ratio of outdoor air ( $W_{OA}$ ) was lower than that of supply air (i.e., set point). The varying speed ( $Spd$ ) of the enthalpy wheel is simulated by using Eqs. (3) to (6) (Jeong et al., 2003) as follows:

$$DFR = 2430.6 \times \frac{(W_{RA}-W_{OA})/(T_{RA}-T_{OA})}{RH_{OA}^2} \quad (3)$$

$$Spd = f(DFR, \varepsilon_{lat}) \quad (4)$$

$$\varepsilon_{lat} = \frac{W_{SA,set}-W_{OA}}{W_{RA}-W_{OA}} \times 100 \quad (5)$$

$$\varepsilon_{sen} = 13.844 \times \ln(Spd) + 38.469 \quad (6)$$

The sensible wheel effectiveness ( $\varepsilon_{SW}$ ) was derived by using Eq. (7). The required amount of heat with respect to the supply air was reclaimed from the exhaust air to satisfy the set point. The sensible wheel effectiveness was also controlled based on the rotation speed of the wheel as described in Eq. (6). In the study, the maximum effectiveness was assumed as 85 % at full-speed operation (Rabbia and Dowse, 2000). The expression for sensible wheel effectiveness is as follows:

$$\varepsilon_{SW} = \frac{T_{SA,set} - T_{SW,in}}{T_{RA} - T_{SW,in}} \times 100 \quad (7)$$

### 3.3 Radiant cooling panel

#### 3.3.1 Ceiling radiant cooling panel

The radiant cooling panel accommodated the additional sensible load of a zone to maintain the room temperature setpoint. In case of the CRCP, chilled water from the chiller was used to accommodate the remaining sensible load of the zone. A single chiller provides a constant flow rate of chilled water that enters the cooling coil in the DOAS and CRCP. The inlet temperature was maintained at 16 °C by mixing the water leaving the cooling coil and CRCP by using a 3-way valve. The constant water flow rate of the chilled water was determined based on the maximum remain heat of the zone during a year in which it was assumed that the maximum leaving water temperature corresponded to 21 °C at CRCP (Uponor, 2013). The energy consumption of the CRCP occurred at the chiller and is described in chapter 3.5.

#### 3.3.2 Thermoelectric module radiant cooling panel

In the TEM RCP case, the TEM was modeled by using a previous developed model (Chen et al., 2013) in Eqs. (8) to (13). The thermophysical properties of a compact TEM ( $\alpha$ : Seebeck coefficient,  $\rho$ : electrical resistivity,  $\kappa$ : thermal conductivity) were calculated by using Eqs. (8) to (10) that involve using maximum heat capacity ( $Q_{max}$ ), temperature of the hot side ( $T_h$ ), maximum temperature difference between the cold and hot sides of the TEM ( $\Delta T_{max}$ ), maximum input current of the TEM ( $I_{max}$ ), uniform cross-sectional area of the entire TEM ( $A$ ) and height of the thermoelement ( $l$ ). With respect to the TEM that was used in the study, the packing fraction of the total TEM area was covered by a thermoelement ( $f$ ) corresponding to 0.5, and the number of thermocouples in a TEM ( $N$ ) corresponded to 127. The expressions are as follows:

$$\alpha = \frac{Q_{max}(T_h - \Delta T_{max})}{NT_h^2 I_{max}} \quad (8)$$

$$\rho = \frac{Af(T_h - \Delta T_{max})^2}{2T_h^2 l} \frac{Q_{max}}{N^2 I_{max}^2} \quad (9)$$

$$\kappa = \frac{l(T_h - \Delta T_{max})^2}{AfT_h^2} \frac{Q_{max}}{\Delta T_{max}} \quad (10)$$

The cold surface temperature of the radiant panel ( $T_c$ ) also corresponded to 16 °C and is the same as that of the CRCP considering the dew point temperature of indoor air. On the hot side, the water from the cooling tower dissipated the rejected heat from the TEM. Therefore, the temperature of the hot side of the TEM ( $T_h$ ) corresponds to the summation of wet-bulb temperature of outdoor air ( $T_{wb, OA}$ ) and the approach of the cooling tower that is assumed two. The lumped thermophysical properties ( $S$ : Seebeck coefficient,  $R$ : Electrical resistivity,  $K$ : Thermal conductivity) of TEM are also estimated by using Eqs. (11) to (13) as follows:

$$S = 2N\alpha \quad (11)$$

$$R = \frac{4N^2l}{Af\rho} \quad (12)$$

$$K = \kappa \frac{Af}{l} \quad (13)$$

The estimated thermophysical properties were used to determine the required input current by using Eq. (14) (Lim and Jeong, submitted). In the equation, it is necessary to define the number of TEMs on the radiant panel (n) based on the maximum remain sensible load of the zone. In the study, it was assumed that twenty TEMs could accommodate the entire sensible load. The cooling load ( $Q_c$ ) corresponded to the remaining sensible load that should be removed by the TEM radiant cooling panel. The input voltage (V) and the amount of heat rejection ( $Q_h$ ) are calculated by using Eqs. (15) and (16) as follows:

$$I = \left\{ \frac{(nAf\alpha^2T_c^2) - \sqrt{(nAf_p\alpha^2T_c^2)^2 - 2\rho(nAf\alpha^2T_c^2)(\kappa\Delta Tnaf + lQ_c)}}{nAf\alpha^2T_c^2} \right\} \times I_{max} \quad (14)$$

$$V = IR + S\Delta T \quad (15)$$

$$P = V \times I = Q_h - Q_c \quad (16)$$

### 3.4 Cooling tower

The cooling tower was simulated with constant water and air flow rates. The water flow rate of the cooling tower ( $\dot{m}_w$ ) was derived based on the maximum heating load of TEM during a year ( $Q_{max, h, TEM}$ ) by using Eq. (17). It was assumed that the range of the cooling tower and heat exchange efficiency of the water block ( $eff_{wb}$ ) corresponded to 10 and 0.8, respectively. Additionally, the liquid to gas ratio (LG ratio) of the cooling tower was determined as 0.1 based on manufacturer data. The air flow rate of cooling tower is calculated from the LG ratio as follows:

$$\dot{m}_w = Q_{max, h, TEM} / (C_{p, w} \cdot Range \cdot eff_{wb}) \quad (16)$$

### 3.5 Electrical chiller

An air-cooled electric chiller model was used in the DOE-2.1 building energy simulation program to simulate the energy consumption of the chiller. This model required a cooling capacity factor (CAPFT), an energy input to cooling output factor in temperature (EIRFT), and an in part load ratio (EIRFPLR) that were derived by using Eqs. (17) to (19). It was assumed that the temperature of the supplied cooling water ( $T_{CWS}$ ) corresponded to 8 °C. The temperature of outdoor air ( $T_{OA}$ ) was varied with respect to weather data from the international weather for energy calculations 2 (IWEC 2). The part load ratio (PLR) is defined in Eq. (20), and the required power of the chiller (P) is derived by using Eq. (21) as follows:

$$CAPFT = f(T_{CWS}, T_{OA}) \quad (17)$$

$$EIRFT = f(T_{CWS}, T_{OA}) \quad (18)$$

$$EIRFPLR = f(PLR) \quad (19)$$

$$PLR = \frac{\text{Required cooling load}}{\text{Capacity of chiller} \cdot CAPFT} \quad (20)$$

$$P = P_{ref} \cdot CAPFT \cdot EIRFT \cdot EIRFPLR \quad (21)$$

## 4 RESULTS

### 4.1 Performance of thermoelectric module radiant cooling panel

As shown in figure 5, the annual performance of TEM-RCP was analyzed in terms of input current and coefficient of performance (COP). The mean input current corresponded to  $2.9 \pm 1.9$ , and the minimum and maximum value corresponded to 0.5 and 11.3, respectively. During the cooling season, the input current increased based on the increase in the remaining sensible load of the zone and wet-bulb temperature of OA. Thus, there was an increase in the temperature difference between the hot and cold sides of the TEM. The COP was calculated by using Eq. (22). The mean value for the COP for cooling (denoted as  $COP_c$ ) corresponds to  $5.6 \pm 3.1$  with minimum and maximum values corresponding to 0.6 and 12.3, respectively. The aforementioned values are considerably high and indicate the possibility of applying the TEM on a radiant cooling panel. However, the COP of the TEM significantly decreased when the temperature difference increased in the cooling season such that it is necessary to define a proper temperature difference with a cooling load in order to use the TEM-RCP. The expression for the COP for cooling is as follows:

$$COP_{cooling} = \frac{Q_c}{P_{TEM}} \quad (22)$$

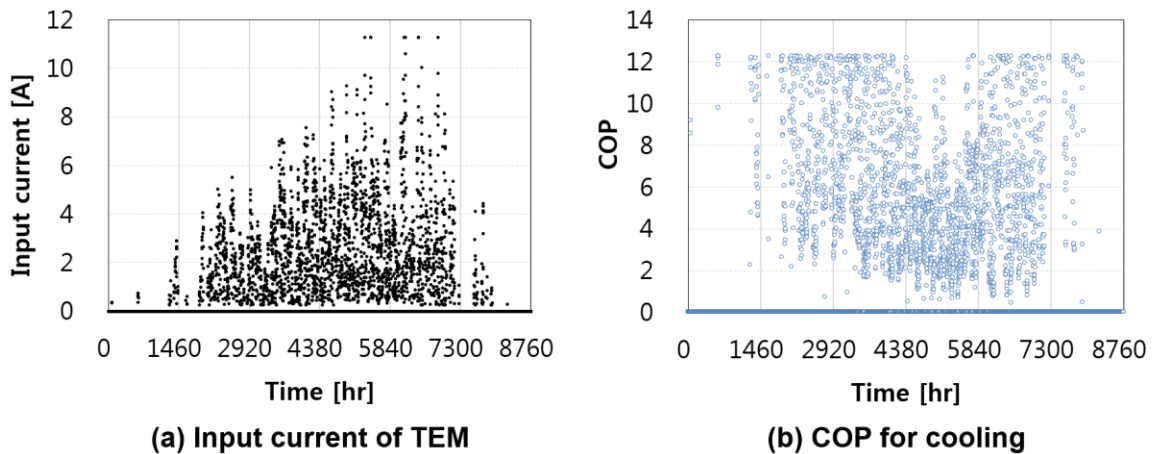


Figure 5: Annual performance of the TEM-RCP in DOAS

### 4.2 Annual energy consumption of systems

The annual electrical energy consumption was compared based on the system and its components (i.e., the chiller, TEM, electrical heating coil, parallel heating unit, pump, and fan)

as shown in Figure 6. The maximum chiller and fan energy among the systems was consumed by the VAV. It is because the DOAS reduced the chiller energy by accommodating the sensible load by using a parallel cooling unit (i.e., radiant cooling panel) and supplying a minimum ventilation air flow rate.

In case of the DOAS CRCP system, a single chiller supplied the entire cooling capacity of the cooling coil and CRCP such that the energy savings of the chiller did not considerably exceed that of the DOAS TEM-RCP system. Conversely, the energy consumption from the TEM occurred in the DOAS TEM-RCP system. With respect to the VAV system, the heating coil also consumed additional energy to reheat the supply air. The heating coil contributed to reducing energy consumption from the parallel heating unit. However, the energy saving was relatively small when compared with energy consumption from the heating coil.

The DOAS TEM-RCP exhibits the maximum pump energy among the systems due to the large water flow rate of the cooling tower. The reason as to why the DOAS TEM-RCP exhibits a water flow rate that exceeds that of the CRCP is because the TEM exhibits heat rejection that exceeds the remaining sensible heat load of the zone. The minimum pump energy was exhibited by the pump in the VAV system because it consists of a single pump with a chiller. Additionally, the fan energy of the DOAS TEM-RCP exceeds that of the DOAS CRCP due to the fan of the cooling tower.

On an overall basis, the total energy consumption of DOAS is lower than that of the VAV system. Furthermore, the DOAS CRCP exhibited the smallest energy consumption among the systems. The findings indicated that the DOAS TEM-RCP displayed energy savings of 44.5 % when compared with that of the VAV system. However, the DOAS TEM-RCP has not replaced the CRCP to date due because it is associated with a low COP and a high amount of heat rejection.

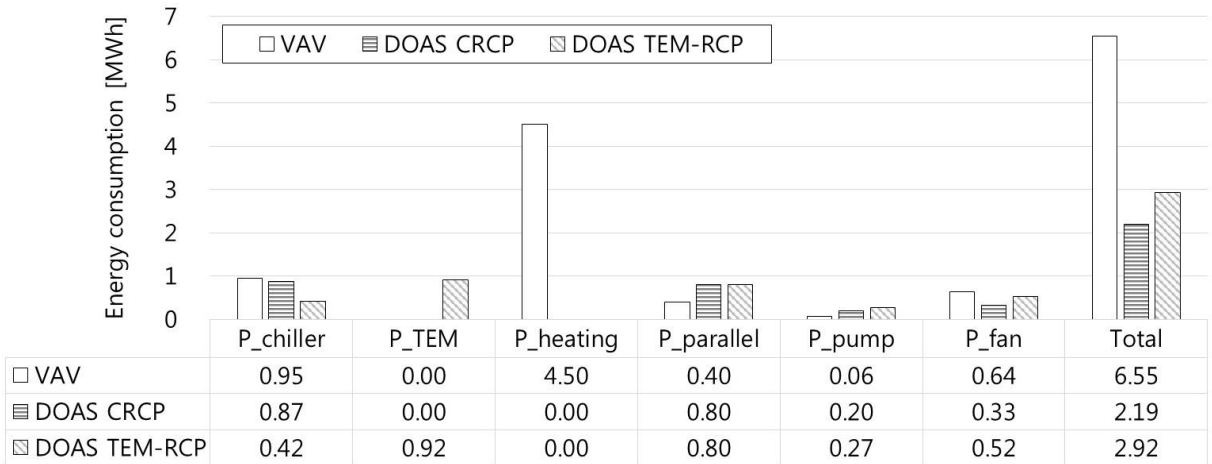


Figure 6: A comparison of the annual energy consumption of systems

### 5 CONCLUSIONS

In this study, DOAS TEM-RCP was suggested and compared with a VAV system and DOAS CRCP with respect to the annual energy simulation. The results indicated that the proposed system reduced annual energy consumption by 44.5 % when compared with that of the VAV system. Additionally, the energy consumption of the TEM-RCP increased by 33 % when compared with that of the DOAS CRCP. This is because the TEM does not display an optimal COP value given high wet-bulb temperatures that prevail in summer. Thus, the proposed system could be limited such that it exhibits a relatively high energy consumption when



compared with that of the DOAS CRCP. However, the DOAS TEM-RCP can easily control the surface temperature of RCP without refrigerants and exhibits an energy saving potential when compared with the VAV system. A future study will include a simulation for an air-cooled TEM-RCP to investigate improved applications of TEM-RCP with DOAS.

## **6 ACKNOWLEDGEMENTS**

This work was supported by a National Research Foundation (NRF) grant (No. 2015R1A2A1A05001726) of Korea and a Korean Agency for Infrastructure Technology Advancement (KAIA) grant (16CTAP-C116268-01).

## **7 REFERENCES**

- Kim, M., Yoon, D. S., Kim, H. J., Jeong, J. W. (2016). Retrofit of a liquid desiccant and evaporative cooling-assisted 100% outdoor air system for enhancing energy saving potential. *Appl. Therm. Eng.* 96, 441–453.
- Tan, G., Zhao, D. (2015). Study of a thermoelectric space cooling system integrated with phase change material. *Appl. Therm. Eng.* 86, 187–198.
- Lee, H.S. (2017). *Thermoelectrics: Design and Materials*. John Wiley & Sons, Inc..
- Jeong, J. W., Mumma, S. A., Bahnfleth, W. P. (2003). Energy conservation benefits of a dedicated outdoor air system. *ASHRAE Trans*, 109(2), 627-636.
- Jeong, J. W., Mumma, S. A. (2005). Practical thermal performance correlations for molecular sieve and silica gel loaded enthalpy wheels. *Appl. Therm. Eng.* 25, 719-740.
- Rabbia, M., Dowse, G. (2000). *Energy recovery ventilation-understanding energy wheels and energy recovery ventilation technology*. Carrier Corporation.
- Uponor. (2013). *Radiant cooling design manual: embedded systems for commercial applications*. Uponor, Inc.
- Chen, M., Snyder, G. J. (2013). Analytical and numerical parameter extraction for compact modelling of thermoelectric coolers. *Int. J. Heat Mass Transf.* 60, 689-699.
- Lim, H., Jeong, J. W. (Submitted). Energy-saving potential of thermoelectric modules integrated into liquid desiccant system for solution heating and cooling. *Energy Convers.*